

The orientation of galaxy dark matter haloes around cosmic voids

Riccardo Brunino,^{1*} Ignacio Trujillo,¹ Frazer R. Pearce¹ and Peter A. Thomas²

¹*School of Physics and Astronomy, University of Nottingham, University Park, Nottingham NG7 2RD*

²*Astronomy Centre, University of Sussex, Falmer, Brighton BN1 9QH*

Accepted 2006 November 10. Received 2006 November 8; in original form 2006 September 12

ABSTRACT

Using the Millennium N -body Simulation we explore how the shape and angular momentum of galaxy dark matter haloes surrounding the largest cosmological voids are oriented. We find that the major and intermediate axes of the haloes tend to lie parallel to the surface of the voids, whereas the minor axis points preferentially in the radial direction. We have quantified the strength of these alignments at different radial distances from the void centres. The effect of these orientations is still detected at distances as large as $2.2 R_{\text{void}}$ from the void centre. Taking a subsample of haloes expected to contain disc-dominated galaxies at their centres we detect, at the 99.9 per cent confidence level, a signal that the angular momentum of those haloes tends to lie parallel to the surface of the voids. Contrary to the alignments of the inertia axes, this signal is only detected in shells at the void surface ($1 < R < 1.07 R_{\text{void}}$) and disappears at larger distances. This signal, together with the similar alignment observed using real spiral galaxies, strongly supports the prediction of the Tidal Torque theory that both dark matter haloes and baryonic matter have acquired, conjointly, their angular momentum before the moment of turnaround.

Key words: methods: statistical – galaxies: formation – galaxies: haloes – galaxies: structure – dark matter – large-scale structure of Universe.

1 INTRODUCTION

The angular momentum of a galaxy plays a central role in determining its evolution and final type. However, understanding the origin and properties of the galactic angular momentum has been one of the key problems in astrophysics in the last five decades. The current ‘standard’ theory for the origin of the angular momentum, within the cosmological framework of hierarchical structure formation, is the tidal-torque theory (hereafter TTT). This theory is based on early ideas from Hoyle (1951) that suggested that the angular momentum of a galaxy arises from the tidal field of neighbouring galaxies. This idea was further developed and quantified by Peebles (1969), Doroshkevich (1970) and White (1984).

The TTT suggests that most of the angular momentum is gained gradually by the protohaloes during the linear regime of the growth of density fluctuations, due to tidal torques from neighbouring fluctuations. Angular momentum grows linearly with time at this early epoch and saturates when the halo decouples from the expanding background at the moment of turnaround. It is assumed that during this phase the baryonic component follows the dark matter distribution and consequently gains a similar specific angular momentum to that of the halo. A subsequent large collapse factor of the baryonic matter to the centre of the halo will explain the centrifugally supported nature of the galactic discs (Fall & Efstathiou 1980).

To first order, the angular momentum of the haloes results from the misalignment between the principal axes of the inertia momentum tensor (I_{ij}) of the matter being torqued and the principal axes of the shear or tidal tensor ($T_{ij} = -\partial^2\phi/\partial x_i\partial x_j$) generated by neighbouring density fluctuations. The leading term of the torque is given by $L_i \propto T_{jk}(I_{jj} - I_{kk})$, where i, j and k are cyclic permutations of 1, 2 and 3. Several aspects of this picture have been confirmed by a number of studies of the angular momentum properties of dark matter haloes both analytically (Heavens & Peacock 1988; Catelan & Theuns 1996) and in N -body simulations (Barnes & Efstathiou 1987; Lee & Pen 2000; Sugerman, Summers & Kamionkowski 2000; Porciani, Dekel & Hoffman 2002a,b).

If \mathbf{I} and \mathbf{T} were uncorrelated (as frequently has been assumed under the argument that the former is local and the latter is dominated by the distribution of the large-scale structure) the direction of the angular momentum in the linear regime should be aligned with the intermediate axis of \mathbf{I} (the direction that maximizes the difference between I_{jj} and I_{kk}). However, Porciani et al. (2002b) have found in their simulations that there is a strong correlation between the \mathbf{I} and \mathbf{T} tensors, in the sense that their minor, major and intermediate principal axes tend to be aligned at the protohalo stage. The strong correlation between \mathbf{I} and \mathbf{T} should produce an angular momentum vector of the haloes that is perpendicular to the minor axis of the sheet they are embedded in (i.e. perpendicular to the direction of the maximum compression of the large-scale structure at that point). However, this last correlation, at least at redshift zero, is expected to be very weak (or totally erased) by non-linear effects

*E-mail: ppxrb@nottingham.ac.uk

(such as exchange of angular momentum between haloes) at late times.

From the observational point of view, Trujillo, Carretero & Patiri (2006) have found that the rotation axes of spiral galaxies located on the shells of the largest cosmic voids lie preferentially on the void surface (in agreement with the expectation for the angular momentum of haloes given in the previous picture). The observational relation could be explained then as a consequence of the spin of the baryonic matter still retaining memory of the angular momentum properties of the haloes at the moment of turnaround (Navarro, Abadi & Steinmetz 2004). It is key, consequently, to explore whether the signal is also found in the haloes of cosmological N -body simulations when we mimic the observational technique. If so, this will strongly support our current understanding of how haloes and baryonic matter have acquired, conjointly, their angular momentum.

Together with the orientation of the angular momentum, the alignment of the shape of the galaxy dark matter haloes ($M < 10^{13} h^{-1} M_{\odot}$) with their surrounding large-scale structure can have important observational consequences. In fact, the shapes of dark matter haloes can affect the coherence of tidal streams (Sackett 1999), can be related to galactic warps (Ostriker & Binney 1989; Debattista & Sellwood 1999; López-Corredoira, Betancort-Rijo & Beckman 2002) or can affect the distribution of the orbits of satellite galaxies (Holmberg 1969; Zaritsky et al. 1997; Sales & Lambas 2004; Agustsson & Brainerd 2006; Yang et al. 2006). In addition, infall of material into the haloes is not isotropic but is expected to be through the filaments where the haloes are embedded. Consequently, the orientation of the dark matter haloes within these structures can affect the characteristics of the galaxy properties previously mentioned.

The alignment of massive (group and cluster) haloes ($M > 10^{13} h^{-1} M_{\odot}$) with their surrounding large-scale structure has been explored in detail (Splinter et al. 1997; Onuora & Thomas 2000; Faltenbacher et al. 2002; Hopkins, Bahcall & Bode 2005; Kasun & Evrard 2005; Basilakos et al. 2006). These works indicate that the major axes of neighbouring galaxy clusters are aligned. A result that is in agreement with the ‘Binggeli effect’ (Binggeli 1982). The origin of these alignments is still under debate and could be associated to infall of material (van Haarlem & van de Weygaert 1993) and/or tidal fields (Bond, Kofman & Pogosyan 1996). Due to the lack of resolution in previous simulations, it is only now that an exploration of the alignment of the galaxy dark matter haloes has become possible (Bailin & Steinmetz 2005, hereafter BS05; Altay, Colberg & Croft 2006, hereafter ACC06; Patiri et al. 2006b, hereafter PA06; Aragón-Calvo et al. 2006). These works suggest that the major axis of the haloes lies along the filaments. The quantification of the strength of these alignments is key to studies of strong and weak lensing where the intrinsic distribution and alignment of galaxy shapes plays an important role in interpreting the signal (see e.g. Croft & Metzler 2000; Heavens, Refregier & Heymans 2000; Heymans et al. 2006).

The aim of this paper is to characterize the alignment of both the shape and angular momentum of galaxy dark matter haloes with their surrounding large-scale structure to an unprecedented statistical level using the Millennium Simulation (Springel et al. 2005). In particular, we will focus our attention on haloes surrounding the largest cosmological voids. Contrary to filaments (which are strongly affected by redshift-space distortion), large cosmological voids are a feature easy to characterize from the observational point of view (Trujillo et al. 2006). In addition, another important advantage of the void scheme is that (because of the radial growth of the voids) the vector joining the centre of the void with the galaxy (halo) is a

good approximation to the direction of the maximum compression of the large-scale structure at that point.

This naturally generates a framework for exploring the alignments of the shape and angular momentum of the haloes with their surrounding matter distribution. Consequently, our work mimics the observational framework to provide an easy interpretation of current and future observations. The large volume sampled by the Millennium Simulation combined with the excellent spatial resolution allows us to conduct this project. This unprecedented statistical power is absolutely crucial if we want to explore signals expected to be very weak like the alignment of halo angular momentum and the large-scale structure.

This paper is structured as follows. Section 2 provides a description of the Millennium Simulation itself, the void and halo samples used and details of how the shapes and spins were measured. Section 3 describes our results and we discuss our findings in Section 4.

2 NUMERICAL SIMULATION

2.1 N -body simulation

The main simulation we have used for this study is the *Millennium Simulation* of Springel et al. (2005). This employs 2160^3 dark matter particles each of mass $8.6 \times 10^8 h^{-1} M_{\odot}$ within a comoving box of side $500 h^{-1}$ Mpc. This simulation was performed in a Λ CDM universe with cosmological parameters: $\Omega_{\Lambda} = 0.75$, $\Omega_{\text{M}} = 0.25$, $\Omega_{\text{b}} = 0.045$, $h = 0.73$, $n = 1$ and $\sigma_8 = 0.9$, where the Hubble constant is characterized as $100 h \text{ km s}^{-1} \text{ Mpc}^{-1}$. These cosmological parameters are consistent with recent combined analyses from *Wilkinson Microwave Anisotropy Probe* data (Spergel et al. 2003) and the 2dF Galaxy Redshift Survey (Colless et al. 2001), although the value for σ_8 is a little higher than would perhaps have been desirable in retrospect. The spatial resolution is $5 h^{-1}$ kpc everywhere inside the simulation volume.

2.2 Void and halo samples

To explore the effect of the large-scale structure on the orientation of the dark matter haloes, we use a similar technique to the one adopted in analysing the orientation of disc galaxies in real observations (Trujillo et al. 2006). To this aim we need, first, to find and characterize the radius of the large voids in the simulation. To speed up the process of finding the voids, we used as an initial guess for the position of the void centres the position of the most underdense particles in the box. To do this, for every dark matter particle in the Millennium Simulation we have estimated the local density by using a standard (Monaghan & Lattanzio 1985; Hernquist & Katz 1989) smoothing kernel averaging over 32 neighbours. We produced a list of the most underdense particles and then radially sorted surrounding particles in distance from these points. In this way the radius of a volume underdense by a factor of 10, centred on the most underdense particle, was calculated. All particles with densities less than 0.035 of the cosmic mean and further than $2 h^{-1}$ Mpc from an even less dense particle were tried as prospective centres. After cleaning this catalogue by removing those positions that lay within a larger void and limiting the size to be larger than $5 h^{-1}$ Mpc in radius, this technique produced 3024 potential void centre candidates. We estimate that this catalogue of potential void centres is greater than 99 per cent complete, given that we tried over 200 000 random centres but only found two additional voids in the last 50 000 (i.e. voids with central densities close to our limit of 0.035).

Once a list of initial positions for searching for voids in the simulation had been created, we used these positions to search for the maximum spheres that are empty of haloes with mass larger than a given value. To conduct this search we follow an algorithm based on a modification of the one presented in Patiri et al. (2006a). The haloes were identified using a minimal spanning tree that links together particles with density exceeding 900 times the background density (Thomas et al. 1998). This is to focus on the core properties. In our case, we have used all haloes with masses larger than $8.6 \times 10^{11} h^{-1} M_{\odot}$ (i.e. those haloes with more than 1000 particles). Using this mass cut we are selecting haloes that contain galaxies with stellar masses similar to the ones used in the observational data. To characterize the final position of the void centres and their radii, we populate a sphere of radius $R = 5 h^{-1}$ Mpc, centred on each initial position, with 2000 random points. For every point in this sphere, we estimate the position of the closest four haloes lying in geometrically ‘independent’ octants. Then we built the sphere defined by these four haloes. This is repeated for all the 2000 random points. As a characterization (position and radius) of the void we choose the biggest empty spherical region generated in the previous step. It is important to stress that the position of the void defined in this way normally does not match the position of the initial guess.

To match the observations we select only those voids whose radius (as measured by the largest sphere that is empty of haloes greater than a given mass) is larger than $10 h^{-1}$ Mpc. This cut produces 2932 voids in our box with a median radius of $14 h^{-1}$ Mpc. To explore the alignments of the haloes we have concentrated only on haloes with masses $8.6 \times 10^{11} h^{-1} M_{\odot} < M < 8.6 \times 10^{12} h^{-1} M_{\odot}$ (i.e. we restrict the sample to galaxy-sized haloes) and located within shells beyond the surface of the voids.

In addition, we have also created a subsample of haloes which contain a disc-dominated galaxy at their centre. These haloes are expected to have had a relatively ‘quiet’ life and have suffered smaller non-linear effects after turnaround such that their spin properties should remain matched to those of the baryonic matter. To select these haloes we have used the semi-analytic galaxy catalogue of Croton et al. (2006). We have created the subsample by selecting the brightest dominant galaxy within $200 h^{-1}$ kpc of our halo centre. We then select those haloes where the semi-analytic code indicates that there is a galaxy brighter than $M_K < -23$ mag that has a bulge-to-total (B/T) ratio $0 < B/T < 0.4$ (i.e. a Milky Way like disc galaxy).

2.3 Halo shapes and spins

To characterize the orientation of the haloes we have determined the orientation of their principal axes and their angular momentum vectors. The principal axes of the halo mass distribution are measured by diagonalizing the inertia tensor,

$$I_{ij} = \frac{1}{N_p} \sum_{k=1}^{N_p} m_k x_{k,i} x_{k,j}, \quad (1)$$

where the sum is over all the particles in the halo N_p , and the coordinates are defined with respect to the centre of mass of the halo of mass M_h . The resulting eigenvalues $M_h a^2/5$, $M_h b^2/5$ and $M_h c^2/5$ are sorted by size, in descending order. The eigenvectors give the directions of the principal axes.

The angular momentum vector of the halo is given by

$$\mathbf{L} = \sum_k m_k \mathbf{r}_k \times \mathbf{v}_k, \quad (2)$$

where the sum is again over all the particles in the halo and \mathbf{r}_k and \mathbf{v}_k are the position and velocity of each particle relative to the centre of mass of the halo.

The uncertainty in the position of the inertia axes and of the angular momentum has been evaluated by comparing these quantities in the same haloes in two different runs that differ by a factor of 20 in resolution. We found that we can measure the orientation of the angular momentum vector with an uncertainty (as provided by the full width at half-maximum of the distribution) of $\sim 14^\circ$ when the number of particles in the (low resolution) halo is larger than 1000. The uncertainties in the inertia axes are 13° for the semimajor and semiminor axes and 20° for the intermediate axis.

Once the angular momentum and the inertia vectors are evaluated, we estimate the cosine of the angle between those vectors and the vector joining the centre of the void with the centre of the halo \mathbf{R} :

$$\mu = \cos \theta = \left(\frac{\mathbf{R} \cdot \mathbf{V}}{|\mathbf{R}| |\mathbf{V}|} \right). \quad (3)$$

3 RESULTS

Fig. 1 shows the probability density distribution $P(\cos \theta)$ of the cosine of the angles between the inertia axes (and the angular momentum) and the vector joining the centre of the void to the centre of the halo. We show the results for two different shells: the shell located at the surface of the void with a width of 5 per cent of the radius (i.e. $1 R_{\text{void}} < R < 1.05 R_{\text{void}}$), and a shell located well beyond the surface of the void at $1.2 R_{\text{void}} < R < 1.4 R_{\text{void}}$. We do this to highlight the effect of moving farther away from the void surface. The dashed line in this figure corresponds to the probability distribution of randomly distributed angles [i.e. $P(\cos \theta) = 1$].

To the best of our knowledge there is no theoretical prediction for the probability density distribution of the angles between the inertia axes and the vector joining the centre of the void to the centre of the halo. For this reason, we have used the following simple analytical expression motivated by the planar symmetry of the problem (Betancort-Rijo & Trujillo, in preparation) to quantify the strength of the signal:

$$P(\mu) d\mu \propto \frac{p d\mu}{[1 + (p^2 - 1)\mu^2]^{3/2}}. \quad (4)$$

If $p = 1$, we obtain the null hypothesis [i.e. $P(\cos \theta) = 1$]. Values of $p > 1$ imply that the inertial axis tends to be aligned with the surface of the shell, whereas $p < 1$ implies that the axis tends to be perpendicular to the void surface. This simple analytical expression produces good fits to the observed distribution with reduced $\chi^2 \lesssim 1$ in most of the cases. The results of our fits are summarized in Table 1.

We find significant alignments of the inertia axes within the shells of the voids. The major axes of the dark matter haloes tends to lie parallel to the surface of the voids (i.e. there is an excess of haloes with large values of θ). For the minor axis the alignment is contrary to the major axis, there is an excess of haloes with the minor axis oriented in the radial direction of the voids. The intermediate axis also tends to lie parallel to the surface of the voids, although the signal is not as strong as in the case of the major axis. As expected, the signal declines in all the cases as the distance from the centre of the voids is increased, although this decline is slow: we still detect a weak signal of alignments of the major and minor axes at distances as large as $\sim 2.2 R_{\text{void}}$ from the void centre. The distribution of angular momentum vectors, however, is compatible with a random orientation.

To test the reliability of our results we have repeated our analysis locating the centres of the voids at random positions within the

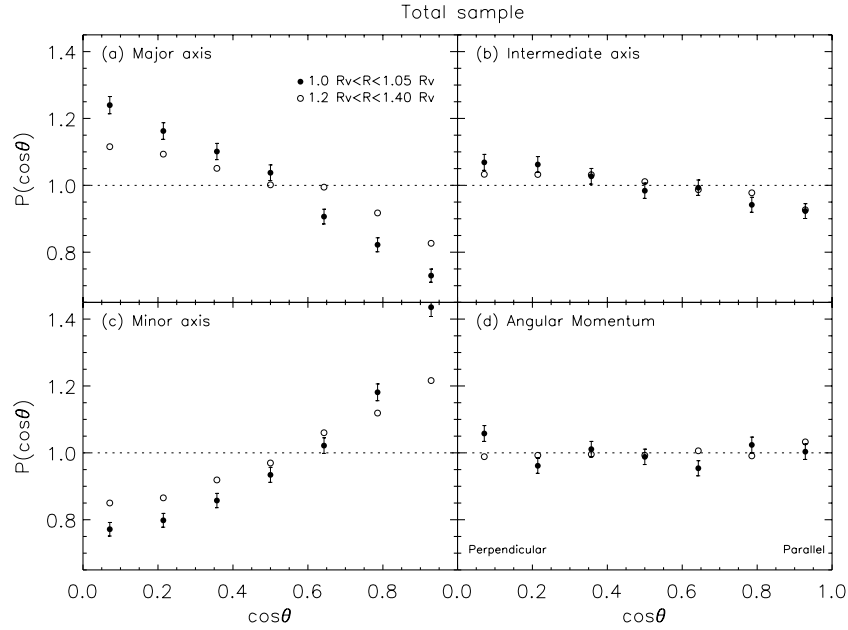


Figure 1. Probability density distribution of the cosine of the angles θ between the inertia axes (and angular momentum) and the vector joining the centre of the voids with the halo centres. The error bar on each bin is the Poissonian error and (to avoid confusion) are only plotted for the innermost shell bins. The null hypothesis (i.e. a sine distribution) is represented by the dashed line.

Table 1. The strength of the alignments on the different shells. To measure the alignment of the inertia axes we have used the parameter p ($p = 1$ in the null case), and c (Lee 2004) in the case of the angular momentum ($c = 0$ in the null case).

Shell R_{void} Units	Maj. A. p	Int. A. p	Min. A. p	A. M. p	A. M. c	Number of haloes
Total sample						
$1.00 < R < 1.05$	1.218 ± 0.012	1.061 ± 0.011	0.778 ± 0.008	1.007 ± 0.010	0.004 ± 0.026	13 128
$1.05 < R < 1.10$	1.165 ± 0.014	1.060 ± 0.013	0.800 ± 0.010	0.994 ± 0.012	-0.014 ± 0.032	8644
$1.10 < R < 1.20$	1.150 ± 0.009	1.057 ± 0.008	0.820 ± 0.007	0.992 ± 0.008	-0.020 ± 0.020	21 567
$1.20 < R < 1.40$	1.111 ± 0.005	1.040 ± 0.005	0.863 ± 0.004	0.989 ± 0.005	-0.033 ± 0.012	60 908
$1.40 < R < 1.80$	1.070 ± 0.003	1.021 ± 0.003	0.914 ± 0.002	0.989 ± 0.003	-0.027 ± 0.007	200 201
$1.80 < R < 2.60$	1.030 ± 0.001	1.011 ± 0.001	0.959 ± 0.001	0.995 ± 0.001	-0.014 ± 0.004	707 760
$2.60 < R < 3.20$	1.011 ± 0.001	1.003 ± 0.001	0.985 ± 0.001	0.998 ± 0.001	-0.004 ± 0.002	1301 720
Disc-dominated subsample						
$1.00 < R < 1.05$	1.172 ± 0.021	1.056 ± 0.019	0.803 ± 0.015	1.062 ± 0.019	0.151 ± 0.046	4212
$1.05 < R < 1.10$	1.156 ± 0.026	1.040 ± 0.023	0.812 ± 0.019	0.994 ± 0.022	0.013 ± 0.059	2587
$1.10 < R < 1.20$	1.148 ± 0.017	1.035 ± 0.015	0.837 ± 0.012	1.003 ± 0.015	0.018 ± 0.038	6366
$1.20 < R < 1.40$	1.098 ± 0.010	1.036 ± 0.009	0.875 ± 0.008	0.991 ± 0.009	-0.029 ± 0.023	17 553
$1.40 < R < 1.80$	1.057 ± 0.005	1.021 ± 0.005	0.920 ± 0.005	0.987 ± 0.005	-0.028 ± 0.013	56 883
$1.80 < R < 2.60$	1.025 ± 0.002	1.012 ± 0.002	0.960 ± 0.002	0.994 ± 0.003	-0.013 ± 0.006	228 198
$2.60 < R < 3.20$	1.013 ± 0.002	1.006 ± 0.002	0.981 ± 0.002	0.999 ± 0.002	-0.002 ± 0.005	370 409

whole volume of the simulation. As expected, we recovered for all the cases a signal which is compatible with the null hypothesis. To run this test we have used exactly the same number of random centres as the number of voids we have. The number of haloes and their distances to the centres of these ‘fake’ voids are similar in this control experiment to the real case.

As stated in the Introduction, any signal of alignment in the angular momentum of the haloes is expected to be erased after the turnaround by non-linear effects. For this reason, if this signal is still present nowadays it should be found in haloes which have had the ‘quietest’ lives since turnaround. To explore this, we have repeated the same analysis as before but this time using the subsample

of haloes with a disc-dominated galaxy at their centre. The results are shown in Fig. 2 and the strength of the signal is quantified in Table 1.

Contrary to the result obtained using the full sample of haloes, the angular momentum vectors of the haloes with a disc-dominated galaxy at their centre tend to lie parallel to the surface of the void. To test the reliability of this signal we have run different statistical tests: the departure of the average (Avni & Bahcall 1980) of $\cos \theta$ from 0.5 (i.e. the expected value in the null hypothesis case) and the Kolmogorov–Smirnov test. Both tests reject the null hypothesis at the 99.8 per cent level. Our results are robust to changes in the ratio B/T ranges selected (i.e. we still find a significant signal for the

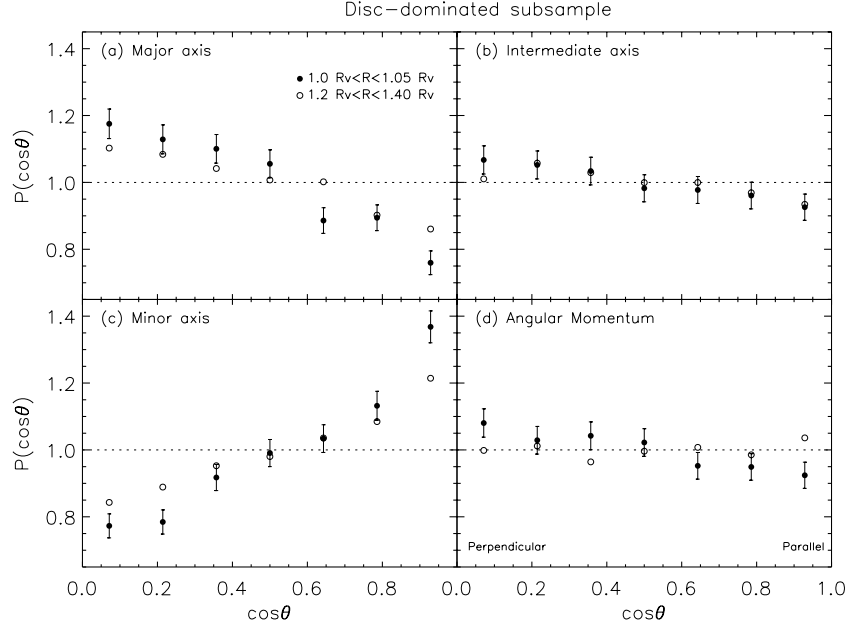


Figure 2. Same than in Fig. 1 but this time using only haloes which contain a disc-dominated galaxy at their centres. Note that using this halo subsample the angular momentum vector tends to lie parallel to the surface of the void.

alignment of the angular momentum including haloes with galaxies with $B/T < 0.6$). In addition, we have also checked that including those haloes contained in our list of voids with $R < 10 h^{-1}$ Mpc do not alter (within the error bars) our results. This is as expected because almost all of our initial void centres produce voids larger than $10 h^{-1}$ Mpc in radius.

It is worth noting that the maximum signal is found when we select a shell of width $1R_{\text{void}} < R < 1.07R_{\text{void}}$. For this case, the null hypothesis is rejected at 99.9 per cent. On the other hand, the inertia axes show the same trends in this subsample as in the previous case using all the haloes.

To characterize the strength of the alignment of the angular momentum we have followed two approaches. We have used (as before) equation (4) and, secondly, we have compared our result with the theoretical prediction for this quantity from Lee (2004) within the framework of the TTT. The strength of the intrinsic galaxy alignment of the galaxies with local shear at the present epoch is expressed as the following quadratic relation (Lee & Pen 2002):

$$\langle L_i L_j \rangle = \frac{1+c}{3} \delta_{ij} - c \hat{T}_{ik} \hat{T}_{kj}, \quad (5)$$

where \mathbf{L} is the halo angular momentum (spin) vector and $\hat{\mathbf{T}}$ is the rescaled traceless shear tensor \mathbf{T} defined as $\hat{T}_{ij} = \tilde{T}_{ij}/|\tilde{\mathbf{T}}|$ with $\tilde{T}_{ij} \equiv T_{ij} - Tr(\mathbf{T})\delta_{ij}/3$, and c is a correlation parameter introduced to quantify the strength of the intrinsic shear-spin alignment in the range of $[0, 1]$. To estimate c we have used the analytical approximation suggested in Lee, Kang & Jing (2005):

$$P(\mu) = \left(1 - \frac{3c}{4}\right) + \frac{9c}{8}(1 - \mu^2). \quad (6)$$

The values of the parameter c we obtain in the different shells are summarized in Table 1. When $c = 1$ the strength of the galaxy alignment with the large-scale distribution is maximum, whereas $c = 0$ implies galaxies are oriented randomly. In the inner shell, we measure in this case $c = 0.151 \pm 0.046$. It is worth noting that the value of c measured in this work is a lower limit of the true value

because it has been evaluated without any attempt to correct for the smoothing produced by the uncertainty in measuring the angular momentum vector of the haloes. Consequently, the strength (and statistical significance) of the observed alignment should be higher. To quantify this effect, we have re-estimated c again but this time using the theoretical prediction convolved with our error function in measuring the angular momentum. After fitting the convolved function to the data, we obtain $c = 0.158 \pm 0.045$.

4 DISCUSSION

In this paper, we have shown that when haloes are selected in order to contain a Milky Way like disc galaxy at their centres the angular momentum of the dark matter halo is oriented preferentially parallel to the surface of the voids. Observationally, the same alignment is detected using the baryonic matter (Trujillo et al. 2006). These two pieces of information are in agreement with the TTT prediction that both the dark and the baryonic matter component have conjointly acquired their angular momentum before the moment of the turnaround. Interestingly, the signal detected in the real observation $c = 0.7^{+0.1}_{-0.2}$ is higher than the one found in the simulations $c = 0.151 \pm 0.046$. This is to be expected taking into account that the signal in the dark matter haloes should be erased by non-linear effects such as exchange of angular momentum between the haloes. Future work, consequently, should explore the strength of the alignment of the haloes at the moment of turnaround. At that early epoch the strength of the signal should be as strong as the one measured using the baryonic component. Porciani et al. (2002b) shows hints that this should be the case by comparing the relation between the halo spin and the linear shear tensor at different redshifts from $z = 50$ to 0.

We have compared our work with previous analysis of the alignment of the inertia axes and angular momentum with their surrounding large-scale structure using different simulations. We concentrate first on the alignment of the angular momentum; using the void framework, neither Heymans et al. (2006) nor PA06 have found a

signal of the alignment of the angular momentum within the shell of the voids. Their results are easily understood taking into account that no pre-selection of the haloes was done in either of these works and that they explored the signal in just one shell of width $4 h^{-1}$ Mpc. In fact, if we mimic their analysis we find $c = -0.014 \pm 0.012$ ($p = 0.996 \pm 0.005$), in agreement with their findings. In the same shell, selecting those haloes with $0 < B/T < 0.45$ produces $c = 0.030 \pm 0.021$ ($p = 1.012 \pm 0.008$). This is a factor of 5 weaker than the signal we find in the closest shell to the void surface. As we have seen in this work, the signal is only significant at the void surface, consequently, taking a wide shell can mask it. In the particular case of Heymans et al. (2006) their mass resolution limit could be another source of concern, since it is a factor of ~ 10 worse than the present simulation.

Comparison with other work is more complicated since the analysis of the alignments is done using a different scheme. BS05 measure the alignment of the angular momentum along filaments. Interestingly, they found that the angular momentum of galaxy mass haloes shows a weak tendency to point along filaments, while those of group and cluster mass haloes show a very strong tendency to point perpendicular to the filaments. The significance and strength of their signal in terms of the c parameter is, however, not quantified. Consequently, the agreement between ours and their work can be done only qualitatively. Porciani et al. (2002b) explored the alignment of massive haloes ($M > 10^{13} h^{-1} M_{\odot}$) between their *final* spin and the *initial* shear tensor at the halo position. They found $c = 0.07 \pm 0.04$. The mass regime explored by these authors and their comparison between an initial and a final property of the haloes prevents us making a direct comparison between their and our measurements of the c parameter. Finally, in a recent paper, Aragón-Calvo et al. (2006), using galaxy mass haloes find that the strength of alignment of their spins in walls is $c = 0.13 \pm 0.02$. This is in excellent agreement with the value reported in this paper.

If we focus our attention on the alignment of the inertia axes, we find that our results are in good agreement with those of BS05, ACC06 and PA06. All these authors find that the tendency of the minor axis to lie perpendicular to large-scale filaments is the strongest of the alignments. It is interesting to note that the strength of these alignments seems to be dependent on the mass of the haloes, being stronger for the most massive (cluster-sized) ones. BS05 and ACC06 suggest that the different strength could be related to fact that most massive haloes receive a larger infall of matter from filaments. This could also help to explain the tendency of the angular momentum of the most massive haloes to be perpendicular to the filaments. In this sense, the cluster mass haloes would acquire most of their current angular momentum from major mergers along the filaments, whereas the angular momentum of the galaxy mass haloes will still have memory of the initial tidal fields.

The alignment of the haloes with their local large-scale structure is not only of interest to constrain models of galaxy formation, it could also be relevant to explain other observational features. For example, the tendency of satellite galaxies to avoid orbits that are coplanar with their host spiral galaxies (known as the ‘Holmberg effect’) found in observations (Holmberg 1969; Zaritsky et al. 1997; Sales & Lambas 2004, but see Agustsson & Brainerd 2006) and in simulations (Zentner et al. 2005; Libeskind et al. 2006). This could be due to the preferential accretion of satellites along filaments, that we have seen are preferentially aligned with the major axis of the host halo.

Finally, it is worth pointing out the potential importance of the alignments we have discussed here to strong and weak lensing studies. In particular, these alignments could contribute to the weak

lensing signal producing a shear-ellipticity correlation (Hirata & Seljak 2004). The degree of contamination that these alignments will produce in the weak lensing surveys should be explored in future work.

ACKNOWLEDGMENTS

We would like to acknowledge very helpful discussions with J. E. Betancort, C. Carretero and V. Springel. We thank the anonymous referee for her/his useful comments. The Millennium Simulation was performed at the MPA by the Virgo Consortium, much of the analysis presented here was completed at the Nottingham HPC centre.

REFERENCES

- Agustsson I., Brainerd T. G., 2006, *ApJ*, 644, L25
 Altay G., Colberg J. M., Croft R. A. C., 2006, *MNRAS*, 370, 1422 (ACC06)
 Aragón-Calvo M. A., van de Weygaert R., Jones B. J. T., van der Hulst J. M. T. 2006, *ApJ*, submitted, preprint (astro-ph/0610249)
 Avni Y., Bahcall J. N., 1980, *ApJ*, 235, 694
 Bailin J., Steinmetz M., 2005, *ApJ*, 627, 647 (BS05)
 Barnes J., Efstathiou G. P., 1987, *ApJ*, 319, 575
 Basilakos S., Plionis M., Yepes G., Gottlöber S., Turchaninov V., 2006, *MNRAS*, 365, 539
 Bingelli B., 1982, *A&A*, 107, 338
 Bond J. R., Kofman L., Pogosyan D., 1996, *Nat*, 380, 603
 Catelan P., Theuns T., 1996, *MNRAS*, 282, 436
 Colless M. et al., 2001, *MNRAS*, 328, 1039
 Croft R. A. C., Metzler C. A., 2000, *ApJ*, 545, 561
 Croton D. J. et al., 2006, *MNRAS*, 365, 11
 Debattista V. P., Sellwood J. A., 1999, *ApJ*, 513, L107
 Doroshkevich A. G., 1970, *Astrofísica*, 6, 581
 Fall S. M., Efstathiou G. P., 1980, *MNRAS*, 193, 189
 Faltenbacher A., Gottlöber S., Kerscher M., Müller V., 2002, *A&A*, 395, 1
 Heavens A. F., Peacock J. A., 1988, *MNRAS*, 232, 339
 Heavens A. F., Refregier A., Heymans C., 2000, *MNRAS*, 319, 649
 Hernquist L., Katz N., 1989, *ApJS*, 70, 419
 Heymans C., White M., Heavens A., Vale C., Van Waerbeke L., 2006, *MNRAS*, 371, 750
 Hirata C. M., Seljak U., 2004, *Phys. Rev. D*, 70
 Holmberg E., 1969, *Ark. Astron.*, 5, 305
 Hopkins P. F., Bahcall N. A., Bode P., 2005, *ApJ*, 618, 1
 Hoyle F., 1951, in Burgers J. M., van den Hulst H. C., eds, *Problems of Cosmical Aerodynamics*, Central Air Documents, Dayton, Ohio, p. 195
 Kasun S. F., Evrard A. E., 2005, *ApJ*, 629, 781
 Lee J., 2004, *ApJ*, 614, L1
 Lee J., Pen U., 2000, *ApJ*, 532, L5
 Lee J., Pen U., 2002, *ApJ*, 567, L111
 Lee J., Kang X., Jing Y. P., 2005, *ApJ*, 629, L5
 Libeskind N. I., Cole S., Frenk C. S., Okamoto T., Jenkins A. 2006, *MNRAS*, submitted, preprint (astro-ph/0607237)
 López-Corredoira M., Betancort-Rijo J., Beckman J. E., 2002, *A&A*, 386, L169
 Monaghan J. J., Lattanzio J. C., 1985, *A&A*, 149, 135
 Navarro J. F., Abadi M. G., Steinmetz M., 2004, *ApJ*, 613, L41
 Onuora L. I., Thomas P. A., 2000, *MNRAS*, 319, 614
 Ostriker E. C., Binney J. J., 1989, *MNRAS*, 237, 785
 Patiri S. G., Betancort-Rijo J., Prada F., Klypin A., Gottlöber S., 2006a, *MNRAS*, 369, 335
 Patiri S. G., Cuesta A. J., Prada F., Betancort-Rijo J., Klypin A., 2006b, *ApJ*, 652, L75 (PA06)
 Peebles P. J. E., 1969, *ApJ*, 155, 393
 Porciani C., Dekel A., Hoffman Y., 2002a, *MNRAS*, 332, 325
 Porciani C., Dekel A., Hoffman Y., 2002b, *MNRAS*, 332, 339

- Sackett P. D., 1999, in Merritt D., Sellwood J. A., Valluri M., eds, ASP Conf. Ser. Vol. 182, *Galaxy Dynamics*. Astron. Soc. Pac., San Francisco, p. 393
- Sales L., Lambas D. G., 2004, MNRAS, 348, 1236
- Spergel D. N. et al., 2003, ApJS, 148, 175
- Splinter R. J., Melott A. L., Linn A. M., Buck C., Tinker J., 1997, ApJ, 479, 632
- Springel V. et al., 2005, Nat, 435, 629
- Sugerman B., Summers F. J., Kamionkowski M., 2000, MNRAS, 311, 762
- Thomas P. A. et al., 1998, MNRAS, 296, 1061
- Trujillo I., Carretero C., Patiri S. G., 2006, ApJ, 640, L11
- van Haarlem M., van de Weygaert R., 1993, ApJ, 418, 544
- White S. D. M., 1984, ApJ, 286, 38
- Yang X., van den Bosch F. C., Mo H. J., Mao S., Kang X., Weinmann S. M., Guo Y., Jing Y. P., 2006, MNRAS, 369, 1293
- Zaritsky D., Smith R., Frenk C. S., White S. D. M., 1997, ApJ, 478, L53
- Zentner A. R., Kravtsov A. V., Gnedin O. Y., Klypin A. A., 2005, ApJ, 629, 219

This paper has been typeset from a $\text{\TeX}/\text{\LaTeX}$ file prepared by the author.